JOURNAL OF Materials CHEMISTRY

Preparation and thermal stability of La_2O_3–Al_2O_3 aerogels from chemically modified Al-alkoxide

Hiroshi Kobayashi, Kiyoharu Tadanaga* and Tsutomu Minami

Department of Applied Materials Science, College of Engineering, Osaka Prefecture University, Sakai, Osaka 599, Japan

La-doped Al_2O_3 aerogels (containing 0.5–10 mol% La_2O_3) were prepared using Al-alkoxide chemically modified with ethyl acetoacetate. The specific surface area of non-doped Al_2O_3 aerogels heat-treated at 1000 to 1200 °C was greatly increased by doping a small amount of La_2O_3. X-Ray diffraction measurements showed that the crystalline phase of La-doped Al_2O_3 aerogels containing 1 mol% La_2O_3 heat-treated at 1200 °C for 2 h was θ-Al_2O_3, while that of non-doped Al_2O_3 aerogels was α-Al_2O_3. The La_2O_3–Al_2O_3 aerogels heat-treated at 1000–1200 °C showed the largest specific surface area at the composition of 1 mol% La_2O_3 with the presence of the θ-Al_2O_3 phase.

Recently, catalyst supports with high thermal stability have been required because of the increase of high temperature reactions such as catalytic combustion at temperatures higher than 1000 °C.[1] However, the specific surface area of conventional γ-Al_2O_3 supports is decreased by sintering at such high temperatures, and thus catalytic activity of the supports is decreased. It has been reported that metal oxides such as La_2O_3 were effective in increasing the thermal stability of conventional γ-Al_2O_3.[2–7]

Aerogels, which are obtained *via* the supercritical drying of wet gels prepared through, for example, the sol–gel method, are porous materials with porosity higher than 90%.[8] They have many characteristic properties owing to the high porosity; for instance, large specific surface area, low refractive index, *etc.* Al_2O_3 aerogels have been investigated as catalysts and catalyst supports.[9] We have already reported the microstructure of Al_2O_3 xerogels and aerogels prepared from Al-alkoxides chemically modified with various stabilizing agents like β-diketones and alkanolamines,[10–12] and shown that Al_2O_3 aerogels have larger specific surface areas at high temperatures than Al_2O_3 xerogels.

In this study, the addition of La_2O_3 to Al_2O_3 aerogels has been investigated in order to further increase the thermal stability. Non-doped Al_2O_3 and La_2O_3–Al_2O_3 aerogels were prepared from Al-alkoxide chemically modified with ethyl acetoacetate. The specific surface areas, pore size distributions, and crystalline phases were measured, and the influences of La_2O_3 content on the thermal stability of aerogels are discussed.

Experimental

Aluminium-tri-*sec*-butoxide (Kanto Chemical Co.), $Al(OBu^s)_3$, was used as a starting material. $Al(OBu^s)_3$ (5.87 g) and isopropyl alcohol (7.16 g, Wako Pure Chemical Industries), Pr^iOH, were mixed and stirred at room temperature for 1 h. Ethyl acetoacetate (3.10 g, Kishida Chemicals), EAcAc, was added to the solution as a stabilizing agent, and the solution was stirred at room temperature for 3 h. Water (1.72 g) diluted with Pr^iOH (7.16 g) containing varying amounts of lanthanum nitrate hexahydrate (Nakalai Tesque), $La(NO_3)_3\cdot 6H_2O$, was added to the solution with stirring for hydrolysis. The sols were kept in closed containers for gelation at 50 °C. The molar ratios of Pr^iOH, EAcAc and H_2O to the total of $Al(OBu^s)_3$ and $La(NO_3)_3$ were set to 10, 1, and 4, respectively. The amount of La_2O_3 was varied from 0 to 10 mol%.

For the preparation of aerogels, the wet gels were aged in Pr^iOH for at least one week at 50 °C and the alcohol was renewed several times to wash out the remaining water in the aging process. The aged wet gels were then supercritically dried in an autoclave at *ca.* 10 MPa at 270 °C, in which the initial pressure of 4 MPa was introduced by nitrogen gas. Xerogels were also prepared as a reference by drying the wet gels at 50 °C for *ca.* 2 weeks for comparison.

The aerogels and xerogels were heat-treated at several temperatures for 2 h. The BET specific surface area and the pore size distribution of these heat-treated gels were measured by the nitrogen adsorption method (Micromeritics, Accusorb 2100). The precipitated crystalline phases of heat-treated gels were identified by X-ray diffraction (XRD) measurements (Rigaku Co., RINT 1000).

Results

Table 1 shows the appearance, bulk density, porosity and specific surface area of non-doped Al_2O_3 and La_2O_3–Al_2O_3 (containing 1 mol% La_2O_3) aerogels without heat treatment. Although some cracks and small shrinkage were observed in non-doped Al_2O_3 aerogels, the appearance is monolithic and translucent. The bulk density of non-doped Al_2O_3 aerogels is *ca.* 0.23 g cm^{-3}, and the porosity calculated from the bulk density is *ca.* 94%. The specific surface area of non-doped Al_2O_3 aerogels is *ca.* 700 m^2 g^{-1}. In the case of La_2O_3–Al_2O_3 aerogels, the appearance is also monolithic and translucent, and the bulk density and porosity are the same as those of non-doped Al_2O_3 aerogels. The specific surface area of La_2O_3–Al_2O_3 aerogels is *ca.* 650 m^2 g^{-1}.

Fig. 1 shows the specific surface area of non-doped Al_2O_3 and La_2O_3–Al_2O_3 (containing 1 mol% La_2O_3) aerogels heat-treated at various temperatures for 2 h. The specific surface area of the La_2O_3–Al_2O_3 aerogels with heat-treatment at temperatures higher than 800 °C for 2 h is larger than that of non-doped Al_2O_3 aerogels, while that of the La_2O_3–Al_2O_3 aerogels without heat-treatment is smaller than that of non-

Table 1 Physical properties of non-doped Al_2O_3 and La_2O_3–Al_2O_3 (1 mol % La_2O_3) aerogels without heat treatment

aerogel	appearance	bulk density /g cm^{-3}	porosity (%)	specific surface area/m^2 g^{-1}
Al_2O_3	translucent	0.23	94	700
La_2O_3–Al_2O_3 (1 mol% La_2O_3)	translucent	0.23	94	650

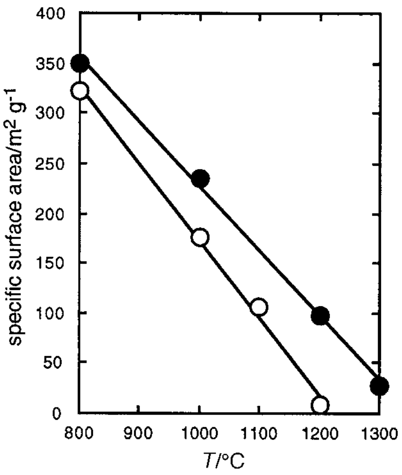

Fig. 1 Specific surface areas of non-doped Al_2O_3 (○) and La_2O_3–Al_2O_3 (containing 1 mol% La_2O_3) (●) aerogels heat-treated at various temperatures for 2 h

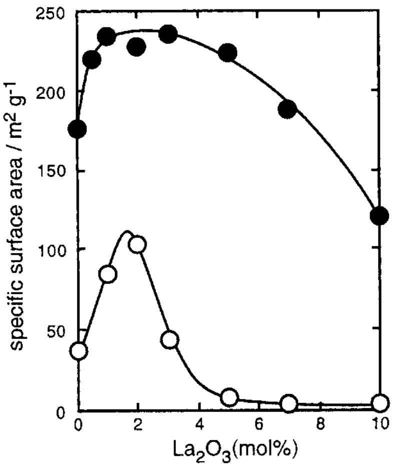

Fig. 3 Specific surface areas of La_2O_3–Al_2O_3 aerogels (●) and xerogels (○) with various amounts of La_2O_3. All aerogels and xerogels were heat-treated at 1000 °C for 2 h.

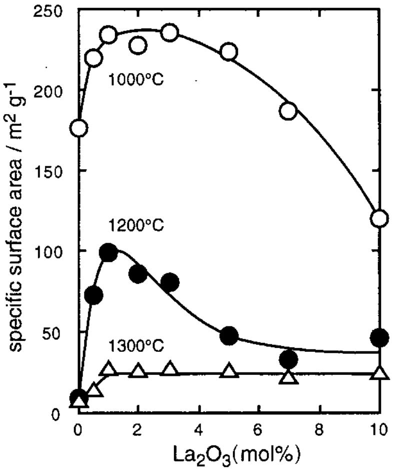

Fig. 4 Specific surface areas of La_2O_3–Al_2O_3 aerogels with various amounts of La_2O_3. All aerogels were heat-treated at various temperatures for 2 h.

doped Al_2O_3 aerogels (Table 1). The specific surface areas of both non-doped Al_2O_3 and La_2O_3–Al_2O_3 aerogels linearly decrease with an increase of the heat-treatment temperature. The extent of decrease for La_2O_3–Al_2O_3 aerogels is smaller than that for non-doped Al_2O_3 aerogels.

Fig. 2 shows the pore size distribution of non-doped Al_2O_3 and La_2O_3–Al_2O_3 (containing 1 mol% La_2O_3) aerogels. The aerogels were heat-treated at 1000 °C for 2 h. Both non-doped Al_2O_3 and La_2O_3–Al_2O_3 aerogels have micropores with pore size of 1–40 nm in radius. The pore size distribution of La_2O_3–Al_2O_3 aerogels is very similar to that of non-doped Al_2O_3 aerogels, while the pore volume of La_2O_3–Al_2O_3 aerogels is larger than that of non-doped Al_2O_3 aerogels. In the range of pore size of 1–2 nm in radius, where pores with these sizes mainly affect the specific surface area, the pore volume of La_2O_3–Al_2O_3 aerogels is clearly larger than that of non-doped Al_2O_3 aerogels.

Fig. 3 shows the specific surface areas of La_2O_3–Al_2O_3 aerogels with various amounts of La_2O_3. The specific surface areas of the La_2O_3–Al_2O_3 xerogels are also shown for comparison. The aerogels and xerogels were heat-treated at 1000 °C for 2 h. The specific surface area of the aerogels are obviously larger than that of the xerogels at any composition. The La_2O_3–Al_2O_3 aerogels and xerogels show maximum specific surface areas at 1–3 mol% La_2O_3. At compositions larger than 3 mol% La_2O_3, the specific surface area of both La_2O_3–Al_2O_3 aerogels and xerogels is decreased with an increase of the amount of La_2O_3.

Fig. 4 shows the specific surface areas of non-doped Al_2O_3 and La_2O_3–Al_2O_3 aerogels heat-treated at 1000, 1200 and 1300 °C for 2 h. As shown in Fig. 3, when the aerogels were heat-treated at 1000 °C, the La_2O_3–Al_2O_3 aerogels show a maximum specific surface area of *ca.* 235 $m^2\,g^{-1}$ at 1–3 mol% La_2O_3 and the specific surface area of non-doped Al_2O_3 aerogel is *ca.* 176 $m^2\,g^{-1}$. For heat-treatment at 1200 °C, the La_2O_3–Al_2O_3 (containing 1 mol% La_2O_3) aerogel shows a maximum specific surface area of *ca.* 100 $m^2\,g^{-1}$, and the specific surface area of the non-doped Al_2O_3 aerogel is only *ca.* 9 $m^2\,g^{-1}$. For heat-treatment at 1300 °C, the specific surface areas of the La_2O_3–Al_2O_3 aerogels are *ca.* 25 $m^2\,g^{-1}$, and show no changes with the amount of La_2O_3.

Fig. 5 shows the XRD patterns of non-doped Al_2O_3 and La_2O_3–Al_2O_3 aerogels. The aerogels were heat-treated at (a) 1000 °C and (b) 1200 °C for 2 h. When the aerogels were heat-treated at 1000 °C, the XRD pattern of the Al_2O_3 aerogel shows the presence of γ- and θ-Al_2O_3 phases. The La_2O_3–Al_2O_3 aerogels are almost amorphous with the addition of more than 1 mol% La_2O_3. When the aerogels were heat-treated at 1200 °C, the α-Al_2O_3 single phase is observed for non-doped Al_2O_3 aerogels. At the composition of 1 mol% La_2O_3, only the θ-Al_2O_3 phase is observed. At compositions of La_2O_3 larger than 3 mol%, the XRD patterns show that the La-β-Al_2O_3 phase, the composition of which is $La_2O_3\cdot 11Al_2O_3$, is present. In the aerogel containing 10 mol% La_2O_3, the XRD pattern shows the presence of a lanthanum aluminate phase, $LaAlO_3$.

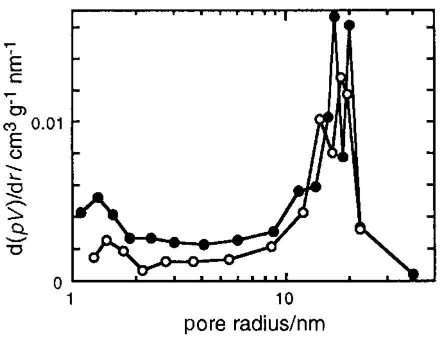

Fig. 2 Pore size distributions of non-doped Al_2O_3 (○) and La_2O_3–Al_2O_3 (containing 1 mol% La_2O_3) (●) aerogels heat-treated at 1000 °C for 2 h

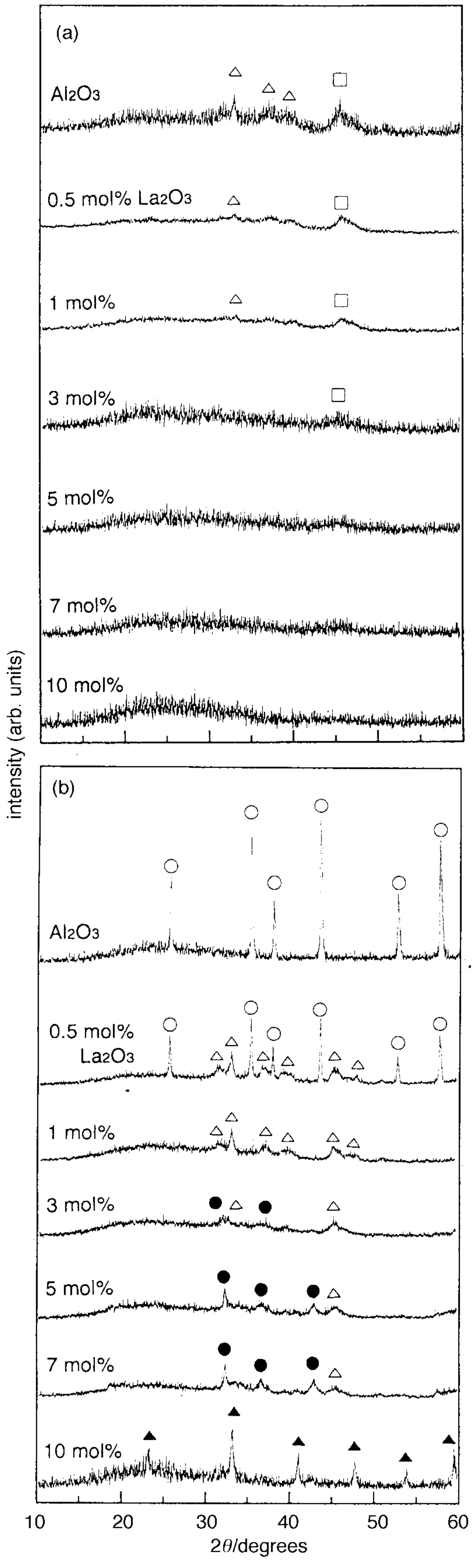

Fig. 5 XRD patterns of La_2O_3–Al_2O_3 aerogels with various amounts of La_2O_3. The aerogels were heat-treated at (a) 1000 °C and (b) 1200 °C for 2 h (△, θ-Al_2O_3; □, γ-Al_2O_3; ○, α-Al_2O_3; ●, La-β-Al_2O_3; ▲, $LaAlO_3$).

Discussion

As shown in Table 1, the specific surface area of the La_2O_3–Al_2O_3 aerogels without heat-treatment is smaller than that of the non-doped Al_2O_3 aerogels. It is assumed that the specific surface area of aerogels as-prepared is affected by the structure of wet gels. In the present study, the gelation time of the La-doped Al_2O_3 gels was longer than that of non-doped Al_2O_3 gels because of the addition of $La(NO_3)_3$. Therefore, it is suggested that the longer gelation time causes the difference in the microstructure between La-doped and non-doped Al_2O_3 gels; gels with longer gelation time have denser microstructure.[11]

The addition of La_2O_3 to conventional γ-Al_2O_3 has been studied by several researchers. For example, Schaper *et al.*[2–4] reported the thermal stability of commercial γ-Al_2O_3 supports, to which La_2O_3 was introduced by the impregnation method. The maximum specific surface area was obtained with the addition of 1–2 mol% La_2O_3. Yamashita *et al.*[6] investigated the addition of rare-earth metal oxides to Al_2O_3 through coprecipitation of aluminium nitrate and rare-earth metal nitrates, and reported that the specific surface area of La-doped Al_2O_3 showed the largest value by the addition of 5 mol% La_2O_3.

As shown in Figs. 1, 3 and 4, the thermal stability of Al_2O_3 aerogels and xerogels prepared by the sol–gel method is increased by the addition of La_2O_3; this is similar to conventional γ-Al_2O_3 supports. As shown in Fig. 2, the pore volume of La_2O_3–Al_2O_3 aerogels is larger than that of Al_2O_3 aerogels. This also shows that the addition of La_2O_3 prevents Al_2O_3 aerogels from sintering. In the present study, the Al_2O_3 aerogels with 1 mol% La_2O_3 showed the maximum specific surface area. This result is similar to samples prepared by the impregnation method.[3] In this method, it is expected that La ions exist on the surface of Al_2O_3 particles. In the sol–gel method, dopants are usually expected to be highly dispersed in the gel matrix. In the present study, Al-alkoxide was used as the Al source, while $La(NO_3)_3$ was used as the La source. Thus, it is assumed that La ions are not dispersed in the whole oxide network of Al_2O_3 particles but in the oxide network of the surface of Al_2O_3 particles, so that the addition of 1 mol% La_2O_3 causes a drastic change of thermal stability.

As shown in Fig. 3, the effect of La_2O_3 addition to aerogel and xerogel appeared in different composition ranges. In aerogels, the increase of specific surface area was observed in the range of La_2O_3 content from 0.5 to 7 mol%. In the case of the xerogels, which had smaller specific surface areas than aerogels, an increase of specific surface area was observed by the addition of 0.5 to 3 mol% La_2O_3. As shown in Fig. 4, aerogels heat-treated at 1200 °C have almost the same specific surface areas and showed similar La_2O_3 content dependence to that of xerogels. These results show that the specific surface area is closely connected to the optimum dopant level, in other words there is an optimum dopant level per unit surface area. If La ions exist on the surface of Al_2O_3 particles, this composition dependence of specific surface area can be explained by the following reason: the La ion concentration per unit surface area shows only slight change with the amount of La_2O_3 for gels with large specific surface areas, whereas it is greatly changed by La_2O_3 content for gels with small specific surface areas.

As shown in Fig. 4, the specific surface area of the La_2O_3–Al_2O_3 aerogels is about 1.3 times larger than that of non-doped Al_2O_3 aerogels when heat-treated at 1000 °C, about 11.1 times at 1200 °C, and about 3.5 times at 1300 °C. This indicates that the degree of increase of the thermal stability of the La_2O_3–Al_2O_3 aerogels is the largest when the aerogels were heat-treated at 1200 °C. Results of XRD measurement (Fig. 5) are compared with those of specific surface area (Fig. 4) for heat-treatment at 1200 °C. It is known that sintering of

Al_2O_3 proceeded *via* surface diffusion,[3] and when densification of Al_2O_3 proceeded with sintering, the specific surface area of Al_2O_3 was rapidly decreased as a result of nucleation and growth of α-Al_2O_3.[4] From the results of Fig. 4 and 5, the specific surface area of non-doped Al_2O_3 aerogels was very small because of the crystallization of the α-Al_2O_3 phase after densification. When 0.5 mol% La_2O_3 was added to Al_2O_3 aerogels, the La_2O_3–Al_2O_3 aerogels have larger specific surface areas than the non-doped Al_2O_3 aerogels. The XRD pattern shows the presence of α- and θ-Al_2O_3 phases and this indicates that the addition of La_2O_3 prevents Al_2O_3 aerogel from sintering and crystallizing to the α-Al_2O_3 phase. The largest specific surface area is observed at 1 mol% La_2O_3 added to Al_2O_3, and the XRD pattern shows only the formation of θ-Al_2O_3. When 3 mol% La_2O_3 was added to Al_2O_3, the XRD pattern of the La_2O_3–Al_2O_3 aerogel shows that the La-β-Al_2O_3 phase is present. Broad diffraction peaks of this crystalline phase indicate that the gels were not well crystallized. Thus, this low crystallinity caused the comparatively large specific surface area. When more than 5 mol% La_2O_3 was added to Al_2O_3, La-containing crystalline phases (La-β-Al_2O_3 and $LaAlO_3$) were detected. Sharp diffraction peaks of these crystalline phases show that the gels were well crystallized in these compositions. This shows that the high crystallinity causes the small specific surface area. As a whole, it is shown that the specific surface area became the largest when the θ-Al_2O_3 phase, a low temperature phase of Al_2O_3, with low crystallinity was present.

Kumar *et al.*[7] reported the mechanism of the improved stability of La-doped Al_2O_3 as follows: the rare-earth cations enter into the interstitial positions of the lattice of transition alumina (γ-, θ-, δ-Al_2O_3, *etc.*) and decrease the oxygen vacancies formed in the neck regions which are the nucleation sites of α-Al_2O_3. In this study, it is expected that La ions exist in the oxide network of the surface of Al_2O_3 particles as mentioned above, and it is expected that there are many defects in the oxide network of the surface of prepared Al_2O_3 gels. Thus, the results of the present study show that La ions should decrease the oxygen vacancy concentration. When the content of La_2O_3 added to the Al_2O_3 aerogels is 0.5–3 mol%, La ions exist in the oxide network of the surface of Al_2O_3 particles and inhibit the sintering of Al_2O_3 *via* surface diffusion. Hence La ions prevent Al_2O_3 aerogels from crystallizing to the α-Al_2O_3 phase. When the content of La_2O_3 added to Al_2O_3 aerogels was larger than 5 mol%, La ions not only prevent Al_2O_3 aerogels from crystallizing but also cause nucleation of La-containing crystals (La-β-Al_2O_3 and $LaAlO_3$) by heat-treatment at *ca.* 1200 °C. Therefore, the thermal stability of Al_2O_3 aerogels was not increased by incorporation of La ions, and also the specific surface areas of Al_2O_3 aerogels were decreased.

Conclusion

We confirmed that the specific surface areas of Al_2O_3 aerogels were greatly affected by the addition of La_2O_3. The addition of a small amount of La_2O_3 to Al_2O_3 aerogels prevented the aerogels from sintering and crystallizing to α-Al_2O_3, and led to large specific surface areas at high temperatures. It was shown that the specific surface area of La_2O_3–Al_2O_3 aerogels became large when the θ- and γ-Al_2O_3 phases, low temperature phases of Al_2O_3, were present. The specific surface area was decreased with an increase of the crystalline phases containing lanthanum, like La-β-Al_2O_3 and $LaAlO_3$. It was found that the addition of 1 mol% La_2O_3 was most effective to give large specific surface areas at high temperatures.

The present study was supported by a Grant-in-Aid from the Ministry of Education, Science, Sports, and Culture of Japan.

References

1 D. L. Trimm, *Appl. Catal.*, 1993, **7**, 249.
2 H. Schaper and L. L. van Reijen, *Proc. 5th Int. Round Table Conference on Sintering*, Porotoz, 1981, p. 173.
3 H. Schaper, E. B. M. Doesburg and L. L. van Reijen, *Appl. Catal.*, 1983, **7**, 211.
4 H. Schaper, E. B. M. Doesburg, P. H. M. de Corte, and L. L. van Reijen, *Solid State Ionics*, 1985, **16**, 261.
5 B. Béguin, E. Garbowski and M. Primet, *Appl. Catal.*, 1991, **75**, 119.
6 H. Yamashita, A. Kato, N. Watanabe and S. Matsuda, *J. Chem. Soc. Jpn. Chem. Ind. Chem.*, 1986, 1169.
7 K.-N. P. Kumar, J. Tranto, J. Kumar, and J. E. Engell, *J. Mater. Sci. Lett.*, 1996, **15**, 266.
8 J. Fricke and A. Emmering, *J. Am. Ceram. Soc.*, 1992, **75**, 2027.
9 Y. Mizushima and M. Hori, *Appl. Catal. A*, 1992, **88**, 137.
10 K. Tadanaga, T. Iwami, N. Tohge and T. Minami, *J. Sol–Gel Sci. Technol.*, 1994, **3**, 5.
11 K. Tadanaga, T. Iwami, T. Minami and N. Tohge, *J. Ceram. Soc. Jpn.*, 1995, **103**, 582.
12 K. Tadanaga, S. Ito, T. Minami and N. Tohge, *J. Non-Cryst. Solids*, 1996, **201**, 231.

Paper 8/00778K; *Received* 28*th January*, 1998